2018

Establishing a Quality Assurance Routine for Digital Imaging

Sulaiman Rana Al
Wright State University

ESTABLISHING A QUALITY ASSURANCE ROUTINE FOR DIGITAL IMAGING

A thesis submitted in partial fulfillment
of the requirements for the degree of
Master of Science

By

RANA AL SULAIMAN
B.S. in Physics, King Faisal University, 2012

2018
Wright State University

WRIGHT STATE UNIVERSITY

GRADUATE SCHOOL

December 13, 2017

I HEREBY RECOMMEND THAT THE THESIS PREPARED UNDER MY SUPERVISION BY Rana Al Sulaiman ENTITLED Establishing a Quality Assurance Routine for Digital Imaging BE ACCEPTED IN PARTIAL FULFILLMENT OF THE REQUIREMENTS FOR THE DEGREE OF Master of Science.

_____
Brent D. Foy, Ph.D.
Thesis Director

_____
Jason A. Deibel, Ph.D.
Chair, Department of Physics

Committee on
Final Examination

_____
Brent D. Foy, Ph.D.
Thesis Director

_____
Steven Cartwright, Ph.D., DABR, DABMP

_____
Sarah F. Tebbens, Ph.D.

_____
Barry Milligan, Ph.D.
Interim Dean of the Graduate School

ABSTRACT

Al Sulaiman, Rana. M.S. Department of Physics, Wright State University, 2018. Establishing a Quality Assurance Routine for Digital Imaging.

In the clinical medical physics field, Quality Assurance (QA) is a fundamental topic to insure patient safety and effective treatment. In recent years, the imaging hardware for diagnostic x-rays has been shifting to fully digital detectors. However, the quality assurance tests for such detectors in the clinical setting is still under development. In the Medical Imaging Department of Kettering Hospital (Kettering, OH), the currently accepted method of performing QA on detectors is to use an extensive set of tests suggested by the manufacturer. This set of tests requires about 90 minutes, which is too long for daily use. The goal of this thesis is to begin the process of developing a more efficient QA routine.

A subset of the manufacturer's tests was selected and used either unchanged or were modified to make them more efficient. To increase confidence that the tests chosen were universally useful, two different models of digital imaging detectors, DX-D 40 and DR 14s from Agfa (Agfa-Gevaert, Mortsel, Belgium), and 4 different x-ray units were investigated. The tests included a uniformity test, a spatial resolution test, a low contrast test, a dynamic range test, and a linearity test. This last test evaluated each detector over

a range of energy and intensity in a short time. The results indicated that the detectors functioned as expected under a wide range of conditions. In addition, these results set a baseline for performance of the detectors that will be useful in regular QA in the hospital setting.

TABLE OF CONTENTS

Page

TABLE OF CONTENTS (Continued)

TABLE OF CONTENTS (Continued)

LIST OF FIGURES

Figure Page

LIST OF FIGURES (Continued)

LIST OF TABLES

ACKNOWLEDGEMENTS

I'm thankful for my parent my father and mother for all their prayers. To my daughter Ashjan in Saudi Arabia for five years of patient since I start studying in United States 2013. To my best friend and sister Lamai. To my roommate and brother Musaed.To my brothers in Saudi Arabia Abdullah and Osama.To my grandfather and grandmother who passed away 2015 and 2016 respectively. They taught me how to be strong. To all friends and family in USA and Saudi Arabia for all their wishes. I would like to thank Dr. Brent Foy for his support and advise. Dr. Steven Cartwright for all his work and support at Kettering Medical Hospital. Dr. Sarah Tebbens for her encouragement. To Jason Deibel Chair of Physics Department for all his support. To my classmate Abdullah and kalel for their supports. To my physics teacher in high school Modi who made me love and chose physics to study. To my best teacher from University of Houston Language and Culture Center Dola Young for all her words, encouragement, and wishes.

I would like to thank the Saudi Arabia Cultural Mission and Saudi Arabia Ministry of Higher Education for full scholarship. I would like to extend my thank for all my advisers from Saudi Arabia Cultural Mission for their supports.

Dedicated

To my parent my father Abdulrahman, my mother Faten

My daughter Ashjan

My sister Lamai

My brothers Abdullah, Musaed and Osama

1. INTRODUCTION

In the medical imaging field, quality assurance (QA) in x-ray imaging is critical to protect patients and employees from the risk of exposure to high dose from the x-ray beams while at the same time maximizing the diagnostic information obtained. Guidelines for quality assurance in medical imaging are determined by professional organizations. The American Association of Physicists in Medicine (AAPM) is a scientific and professional organization which provides guidance to assure accuracy in the delivery of the radiation dose during each x-ray exposure for both diagnostic and therapeutic procedures. State regulatory agencies are also responsible for quality assurance in hospitals in the United States of America. Finally, each hospital has a radiation safety department that maintains QA for medical imaging by following the above regulatory guidelines.

X-ray imaging has undergone multiple changes in technology over the years. Originally, films were used to detect the image. Later, computed radiography (CR) was used. Recently, full digital radiography (DR) is becoming more common. However, the regulatory guidelines for DR detectors have not been fully established at the national level. Therefore at this point in time, each hospital must create its own QA routine for DR detectors.

At Kettering Hospital (Kettering, OH), the primary basis for a set of QA tests is provided by the DR detector manufacturer. This set of manufacturer's tests are designed

to initially commission the DR detector. These tests are quite comprehensive, and consequently require a great deal of time, around 90 minutes. This makes it unsuitable for routine use. The goal of this thesis is to investigate a subset of these manufacturer tests, as well as develop new tests that can validate and investigate DR detector performance in a more efficient manner. The manufacturer's QA protocol involved eight separate tests. In an attempt to reduce the time required to conduct QA for x-ray detectors, we propose a set of five tests that can provide a similar amount of QA information in a more efficient manner.

Two digital detectors, DX- D40, and DR 14s, both from Agfa (Agfa-Gevaert, Mortsel, Belgium) were investigated in combination with 4 different x-ray machines. Studying the DR detectors under a variety of conditions should reveal whether the chosen set of tests are valid under various conditions.

2. BACKGROUND

2.1 X-ray Production

As highly energetic electrons interact with matter, electromagnetic radiation is produced. In the medical field, x-ray machines are used to produce x-rays. These machines in general, contain an x-ray tube, generator, and collimator. The x-ray tube contains the source of electrons (cathode), and a high atomic number material (anode) which are both located within an evacuated tube (Figure 1).

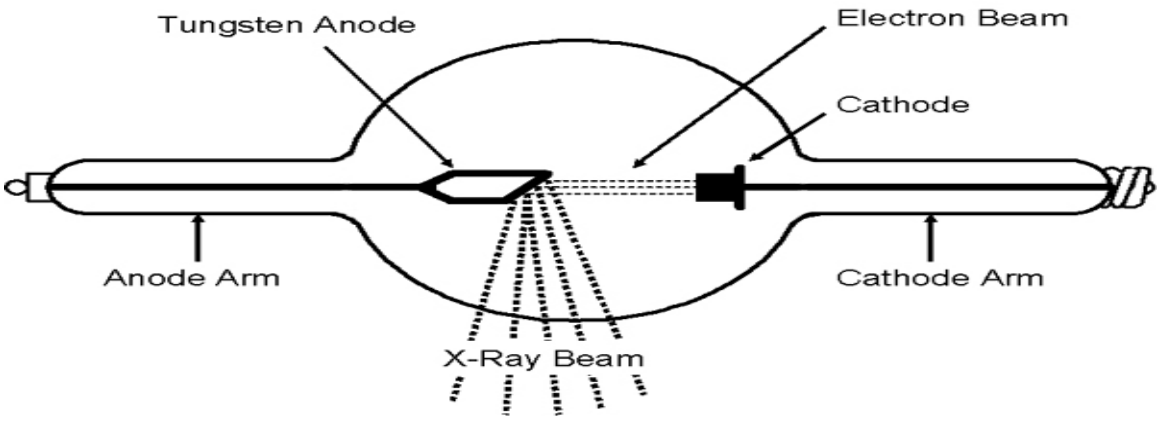

Figure 1: X-ray Tube. Source: Oak Ridge Associated Universities

A current source supplies current to the cathode, and a greater current leads to the release of electrons from the cathode at a greater rate. A voltage source is applied between the cathode and anode creating a potential difference. There are three main quantities which can be chosen by the operator when running an x-ray machine: tube voltage, tube current, and exposure time which measured in kV, mA, and s. Usually, the

product of tube current and exposure time is used as a single quantity and measured in mAs which is proportional to the number of electrons that are generated in the x-ray tube.

The range of potential difference applied between the cathode and anode is 20 – 150 kV. As a consequence, the electrons from the cathode reach the anode with an energy equal to the product of potential difference and the amount of charge on electron. A large fraction of these electrons collide with the anode target and are converted to heat. However, a fraction is decelerated by the strong attractive force of target nuclei, resulting in a loss of kinetic energy. This process leads to the creation of photons (x-rays) in a phenomenon is called bremsstrahlung radiation (Figure 2).

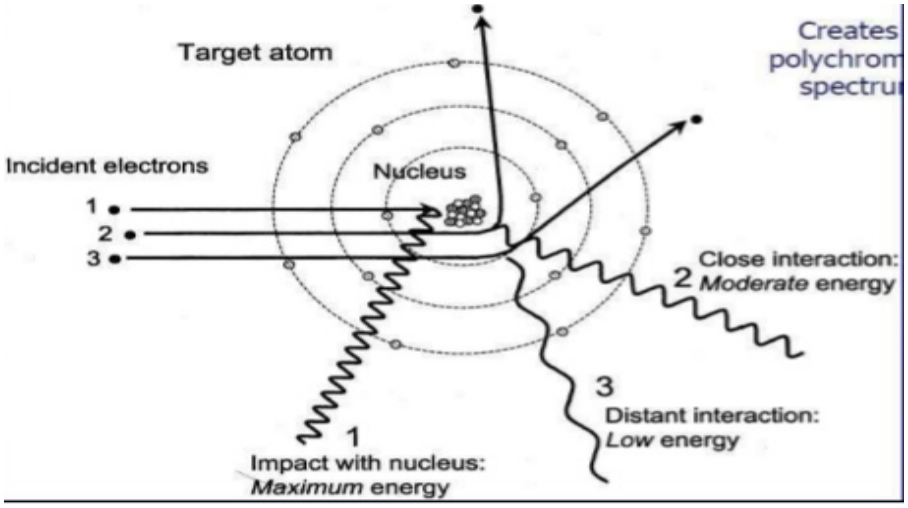

Figure 2: Bremsstrahlung radiation. Source: The essential physics of medical imaging by J.T. Bushberg.

The x-ray photon energy of bremsstrahlung radiation is a spectrum of different energies (Figure 3).

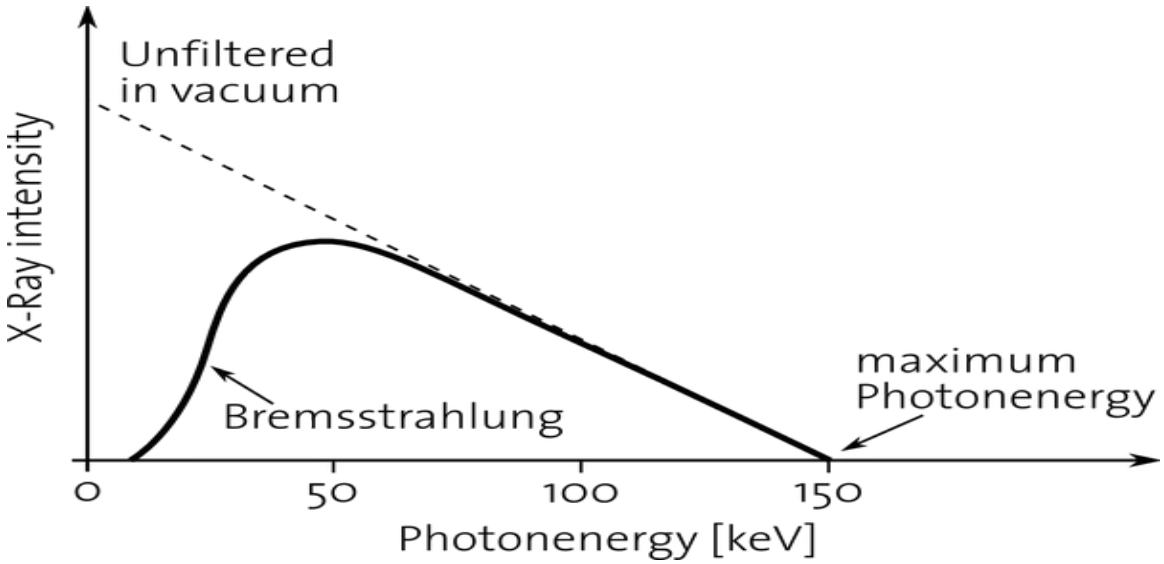

Figure 3: The bremsstrahlung energy distribution for a 150 KV. Source: The essential physics of medical imaging by J.T. Bushberg.

The dotted line represents the unfiltered radiation where the low energy radiation is still in the spectrum, however the bold line represents the filtered spectrum of energy. In a filtered spectrum, the average photon energy is usually estimated to be equal to a third of the maximum energy.

In order to create high quality images and reduce patient dose, a filter made of aluminum or copper or both materials is usually used. Aluminum (Al) and copper (Cu) are used because they have a high atomic number. By placing the filter in the direct path of x-ray beam, the beam gets harder. A harder beam is one that has fewer low energy photons. The filter absorbs low energy x-ray photons before they reach the patient or the

image receptor (IR). Filter thickness is measured in mm. In x-ray radiography practice, the amount of filtration for an x-ray unit is based on voltage potential (kV) that is chosen for the image, with greater thicknesses used for greater kV settings. Using a filter reduces dose to the patient because low energy photons are primarily absorbed by the skin of the patients and provide little enhancement of the image of interior structures, and thus they are a source of unnecessary dose.

Collimation is also used in x-ray imaging. A collimator is a set of x-ray opaque materials that restrict the x-ray beam to only strike the desired region. In general, this is used to make sure that the beam doesn't extend beyond the size of the detector. Again, this reduces unnecessary dose to the patient.

The phrase kilovoltage peak (kVp) will be used in this thesis. It refers to the maximum photon energy (Figure 3), and is also equal to the voltage set on the x-ray machine between cathode and anode. The quality of image depends on the amount of energy reaching the IR. It is essential to adjust mAs and kVp carefully before imaging. The mAs has a direct affect on image brightness. However, in order to create a range of contrast, different energy levels are needed. To ensure high image quality (less noise), the kVp is chosen to penetrate the object and the mAs is chosen to give enough image brightness.

2.2 X-Ray Detection

2.2.1 Film

For many years, x-ray imaging relied on film that consists of 0.2 mm of a polyester base coated with photographic emulsion. There are many types of film: screen-film, direct – exposure film, and special application film. Film requires a clean environment in order to reproduce all information (Bushong,2013). Processing the film requires three steps. First, enhance the film in an alkaline solution to fix the film. Second, utilized an acid solution to protect the film from light due to silver ions stability effected (Haus, 1997). Third, wash the film in water. Finally, dry the film by using hot air (Williams,2008).When developed, the light transmission of the film is called the optical density. Contrast on film is the difference in optical density (OD) $D_2 - D_1$ between two regions. Film provides high spatial resolution which is the ability to image two separate objects and visually distinguish one from the other (Bushong,2013)

When handling and storing film, it is essential to exercise care because it is a sensitive radiation detector. Artifacts can occur due to improper handling. Heat and humidity, light, and radiation have a negative impact on the film (Bushong,2013).

2.2.2 Computed Radiography

In the 1980s, x-ray imaging moved to computed radiographic (CR) systems, which have several advantages over film. One is that it "produces images in a digital format, a format that can be stored and processed in a computer and displayed on a

monitor" (Williams, 2008). The image size of a digital image is determined by dividing the image into a matrix of pixels or individual cells (Williams, 2008).

In CR, the image data is recorded on a photostimulable phosphor plate. In order to release this trapped energy, laser light is shone on to the plate, and the resulting energy release is recorded. The amount of energy released is proportional to the x-ray energy that reached the plate. This method however has disadvantages such as the time and effort that it takes to complete the process, like removing the cassette from the machine (Williaas,2008). CR image spatial resolution is less than film due to many factors and the pixel size which varies depending on the plate size. Another factor that effects spatial resolution is the scatter of the laser light that arises with the thickness of the phosphor (Williams, 2008).

2.2.3 Digital Radiography

In the 1990s, full digital radiography (DR) was introduced. The digital detector uses a thin-film transistor (TFT) that has a scintillator layer and a light-sensitive TFT photodiode (L. Lanca, 2013). The structure of DR is shown in Figure 4.

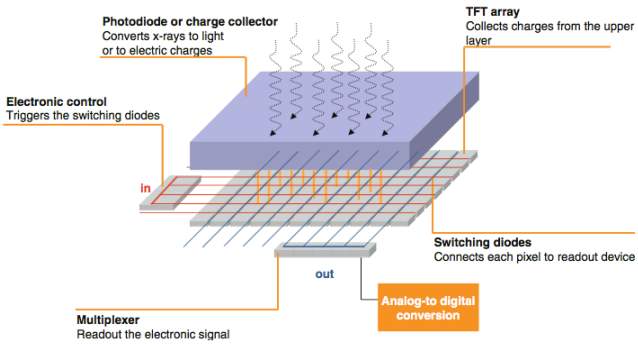

Figure 4 Digital imaging structure (flat panel) Source: Digital Imaging Systems for Plain Radiography by L. Lanc ,a and A. Silva,

In DR detectors, the top layer is CsI or gadolinium oxisulphide (Gd_2O_2S) which converts the x-ray photon to light. This scintillator material can be structured or unstructured (Figure 5). The unstructured scintillator reduces spatial resolution because the light can scatter widely. Structured scintillators reduce the lateral scattering of light photons (L. Lanca,2013). After the scintillator converts the x-ray to light, then comes the second stage when light is converted into an electric charge. The light is converted by an a-Si photodiode array. This photodiode is integrated into the TFT layer (L. Lanca,2013), which permits readout of the location (pixel) where the charge was created.

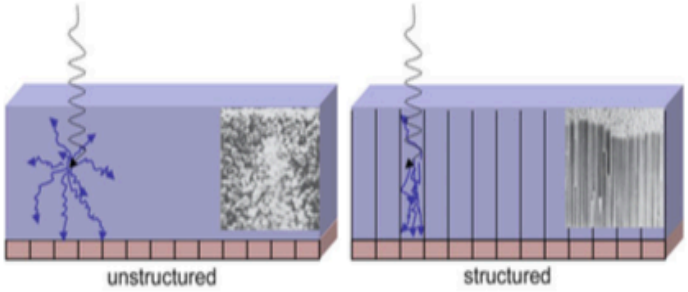

Figure 5 Schematic of an unstructured and structured scintillator source Digital Imaging Systems for Plain Radiography by L. Lanc ¸a and A. Silva

Imaging by this digital process makes images easy to store and access. After imaging, the image takes less than five second to display on computer screen. For the radiologist, DR is a convenient environment because the setup is automatic and there is no need to process image manually. As with CR, the spatial resolution is less than with film. But there is an advantage with both CR and DR because digital images displayed on a monitor can be adjusted (clipping levels, etc.) to make even x-ray images that were obtained under suboptimal conditions more informative.

2.3 X-ray Image Quality

It is fundamental for the radiologist to have a high-quality digital image in order to make accurate diagnoses. There are image quality concepts that the radiographer should understand because they play a role in influencing the usefulness of radiographic images (Bushing,2013). These are spatial resolution, contrast, noise, and dynamic range.

2.3.1 Spatial Resolution

Spatial resolution is the ability to image two separate objects and visually distinguish one from the other. In other words, spatial resolution is the ability to distinguish two objects close together. It is measured as the smallest spacing of lines that can be distinguished under optimal (high contrast) conditions. Resolution has units of Line Pairs per mm (Lp/mm).

2.3.2 Contrast

Contrast is the ability to distinguish small differences in image intensity. It is a visual evaluation of locations with varying intensity compared to background. Contrast can be affected by the kV setting. For example, a high kV setting makes photons more energetic and so they are more likely to reach the digital detector, regardless of what tissues were in the way. Thus, the image loses contrast. On the other hand, a low kV means less photons penetrate to detector, which can increase contrast, but at a price of increased noise (see below).

2.3.3 Noise

Noise is random variation in image intensity, from pixel to pixel, that isn't due to actual differences in absorption by the object (or person) being imaged. Variations due to the object being imaged are called "signal". Noise processes are usually random in nature. There are several sources of noise, and the main two sources are electronic and

quantum noise. Electron noise is due to random processes in the electronics of the detector and are generally negligible for x-ray imaging. The more important noise process is quantum noise, which is related to the number of photons that reach the detector. As the number of photons used for imaging increase, the clarity of image also increases. However, the patient dose is also affected by increasing the photon number, so a tradeoff is always necessary.

Note that the absolute value of noise, usually measured as a standard deviation of pixel intensities in a homogeneous region, increases as the number of photons reaching the detector increases. However, the noise only increases as the square root of the number of photons, because photons follow Poisson statistics. However, the "signal" (due to actual patient tissue differences) increases linearly with the number of photons being used. Therefore, the signal-to-noise ratio goes up with a greater number of photons.

2.3.4 Dynamic Range

Dynamic range can be defined as the total number of intensity levels between "dark" and "light" regions. For example, a device with a small dynamic range could have the dark region = 80 (arbitrary intensity units), and the light region = 60. A device with a large dynamic range would have the dark region = 2000 and the light region = 200. In the small dynamic range case, there are only 20 "levels" between dark and light, and the ratio is only 80/60 = 1.33. In the high dynamic range case, there are 1,800 levels, and the ratio

is 2000/200 = 10.0. More levels and a bigger ratio makes it easier to detect differences between similar tissues. A large dynamic range also increases the ability to digitally "adjust" the display of the image to emphasize features.

2.4 Exposure

In a strict radiation physics sense, exposure is defined as the charge in Coulombs of ion pairs created by a beam per kg of material, usually air. Thus it represents the potential to deposit radiation energy into a material (or patient). However in x-ray imaging, the term exposure, while clearly related to the above definition, refers more to whether the image detector has received the "right" amount of energy (photons) so as to make the image quality as high as possible. For example, an image can be overexposed if there are too many photons that penetrate to the digital imaging receptor. Multiple factors affect the exposure: x-ray tube kV affects photon penetration through the patient, x-ray machine current (mA) determines the rate of photon emission, exposure duration (s) is linear with the number of photons reaching the detector, patient thickness, and source-to-detector distance.

With film, a proper exposure was relatively straightforward to identify. If exposure was too high, the film would be uniformly dark. If exposure was too low, the image would be noisy and too light. With digital detectors, proper exposure is more complicated. Because one can post-process the digital image, it is possible to obtain reasonably good images over a wide range of exposures, wider than was possible for

film. However, there are still physics issues that define the optimal exposure. Namely, too much exposure (too many photons) eventually reduces contrast, and too little exposure (too few photons) leads to increased noise.

All digital detectors provide a report as to the exposure obtained for each image, as well as the optimal range of exposures. Each manufacturer uses a different system for reporting exposure.

2.5 Current State of QA for X-ray Digital Imaging Detector

Digital imaging plates are still new in the x-ray imaging field. The American Association of Physicists in Medicine (AAPM), forms task groups of academic personnel to evaluate best practices to assure accuracy and safety for both diagnostic and therapeutic procedures. Because these digital imaging plates are new, physicists are still working to establish a QA routine for these DR detectors. Task Groups have been working on QA for DR imaging detectors. They test contrast, noise, spatial resolution. Task Group 150, titled "Acceptance Testing and Quality Control of Digital Imaging Units", seeks to determine a set of tests for digital imaging detectors, and tackles the issue from a physicist's perspective. Task Group 151, titled "Ongoing Quality Control in Digital Radiography", seeks to identify issues with imaging systems and deals with the subject more from the point of view of the x-ray technologist.

3. MATERIALS AND METHODS

3.1 Materials

3.1.1 X-Ray Units

Four different x-ray machines were used in for this project. One was a stationary unit and the other three were portable units which will be labeled A, B, and C (Figures 6 and 7). All of the units were manufactured by General Electric (GE, Madison, WI). These x-ray units were chosen because they are convenient and available at Kettering Medical Center. Multiple units were used because it is important verify that the QA tests being developed are useful for multiple types of x-ray machines and under multiple operating conditions. The range of operating conditions possible for these x-ray units is presented in Table 1.

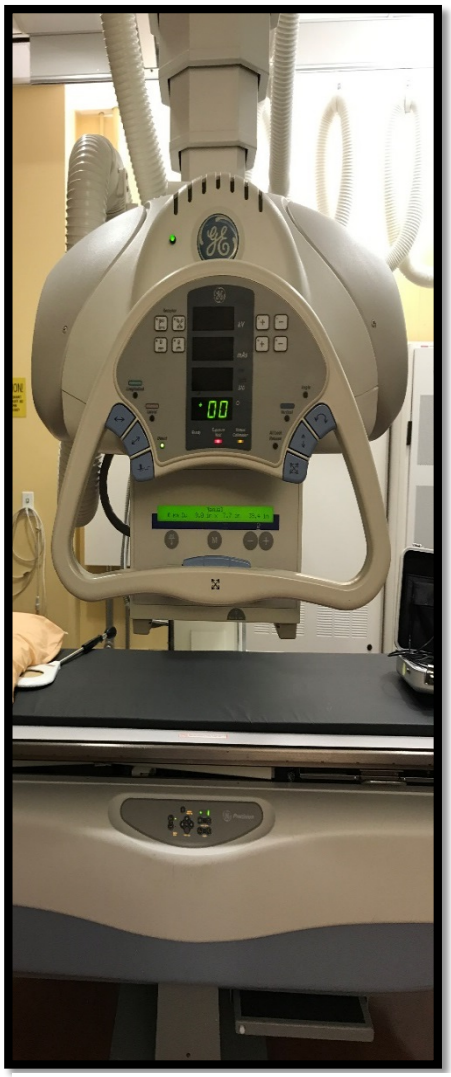

Figure 6 Stationary x-ray unit in room 7

Figure 7 Portable x-ray unit

Parameters	Stationary Unit	Portable Unit
Voltage (kVp)	50-150	50-130
Tube Current (mA)	10-1200	10-1000
Exposure Time (s)	0.001-10	0.001-10

Table 1 X-ray units voltage (kVp), tube current (mA), and exposure time (s)

3.1.2 Solid State Detector

A solid state detector was used to measure dose in μGy for calibration purposes for one of the tests. The Xi detector system manufactured by (Unfors, now RaySafe) was used in this project. It consists of the solid state detector itself (Figure 8) and a readout system (Figure 9).

Figure 8 Calibration Systems from Unfors Xi

Figure 9 Solid State Detector

3.1.3 Digital Imaging Detectors

In this project, two digital detectors were used: the DX-D 40, and the DR 14s, both manufactured by AGFA Health Care (Figures 10 and 11). These digital detectors can be used with any X-ray system (conventional and mobile digital) (Agfa,2016). Table 2 indicates the technical specifications for these digital detectors.

Figure 10 Digital imaging detector the DX-D 40. Source Agfa manufacture manual

Figure 11 Digital imaging detector DR 14s. Source Agfa manufacture manual

Pixel pitch refers to the distance from the center of one pixel to the center of the next pixel. The pixel pitch for DX-D 40 and DR 14s are 140 µm and148 µm respectively. Digital detector DX-D 40 is thus capable of higher spatial resolution than DR 14s due to this lower pixel pitch value. Accordingly, the spatial resolution capability for the DX-D 40 is 3.5 lp/mm, while for the DR 14s it is 3.37 lp/mm. The energy range of 40 – 150 kVp was the same for both digital detectors.

DETECTOR	DX-D 40	DR 14s
Detector type	Amorphous Silicon with TFT	Amorphous Silicon with TFT
Conversion screen	CsI and GOS	CsI (Cesium Iodide) and GOS (Gadolinium oxysulfide)
Pixel pitch:	140 µm	148 µm
Active pixel matrix:	2560 x 3072 pixels	2400 x 2880 pixels
Active area size:	14.09 x 16.92 in (358.4 x 430.1 mm)	430 mm x 350 mm
Effective pixel matrix:	CsI: 2548 x 3060 GOS: 2560 x 3072	2330 x 2846 pixels
Grayscale:	14 bit	16 bit
Spatial Resolution	Min. 3.5 lp/mm	Min. 3.37 lp/mm
Outer dimensions:	5.11 x 18.11 x 0.59 in (384 × 460 × 15 mm) (ISO 4090)	
Weight:	CsI: 7.49 lbs (3.4 kg)	2.8 kg including battery
Energy Range Standard:	40 – 150 kVp	40 – 150 kVp

Table 2. Technical Speciation and system control unit for digital detectors DX-D 40 and DR 14s

3.1.3.1 Pixel value index (PVI)

The Pixel Value Index (PVI) is an output from each pixel of the detector. The actual value is the result of a proprietary calculation by the detector manufacturer. When an image is displayed on a monitor, the PVI corresponds to the intensity for each pixel. Note that PVI, and also therefore the displayed intensity in images, is not strictly proportional to the exposure that occurred at each pixel. The goal of converting pixel

exposure to PVI is so that the resulting images are more useful to humans, especially radiologists. As will be shown in the results section, we have found that in fact PVI is proportional to the logarithm of exposure. Partly this mimics the image intensity that appears in traditional x-ray films. Also, these logarithmic exposure values correspond to the way the human eye detects changes in intensity.

3.1.3.2 Noise Values

Another output from the digital detector is an evaluation of the signal-to-noise ratio for a defined region. When one evaluates a region with multiple pixels, the software can calculate both the average PVI and the standard deviation of underlying exposure values for all the pixels in the defined region. In order to make the evaluation of noise levels under different exposure conditions easier, the average signal (the exposure) is set to a standard value. Thus a higher "Noise" value reported by the software indicates a lower signal-to-noise ratio, since signal is always scaled to a fixed value.

3.1.3.3 Exposure Index (EI)

Exposure index is directly propositional to energy incident on the detector. It can be calculated over a small area or over the entire detector. EI indicates if an area is over- or under-exposed.

3.1.4 Normi 13 phantom

The test object Normi 13 (T42023) dimensions are 300mm X 300mm X 10mm.The phantom contains a Cu filtration. The phantom contains various regions for conducting different kinds of tests. A photo is shown in Figure 12, and a schematic identifying the regions is shown in Figure 13. These regions will be referred to when describing the actual QA tests performed.

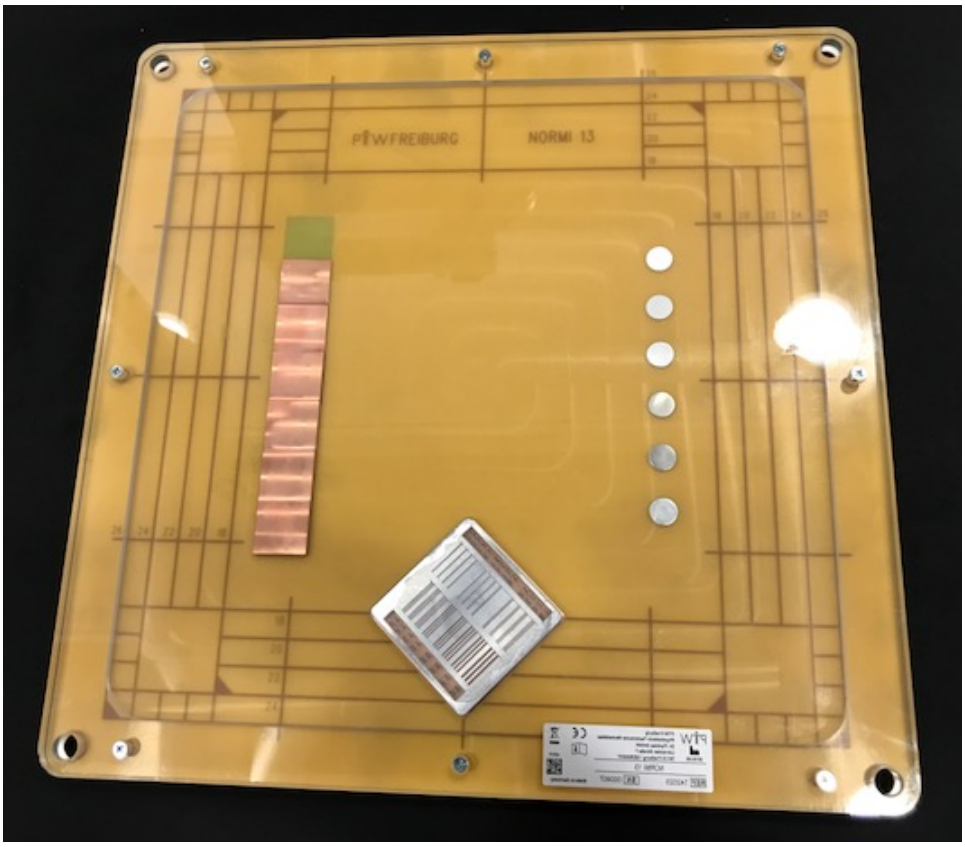

Figure 12 PTW NORMI 13 phantom (front view) suggested by Agfa manufacture to conduct exposure index, pixel vale, contrast resolution, and spatial resolution, and contrast resolution.

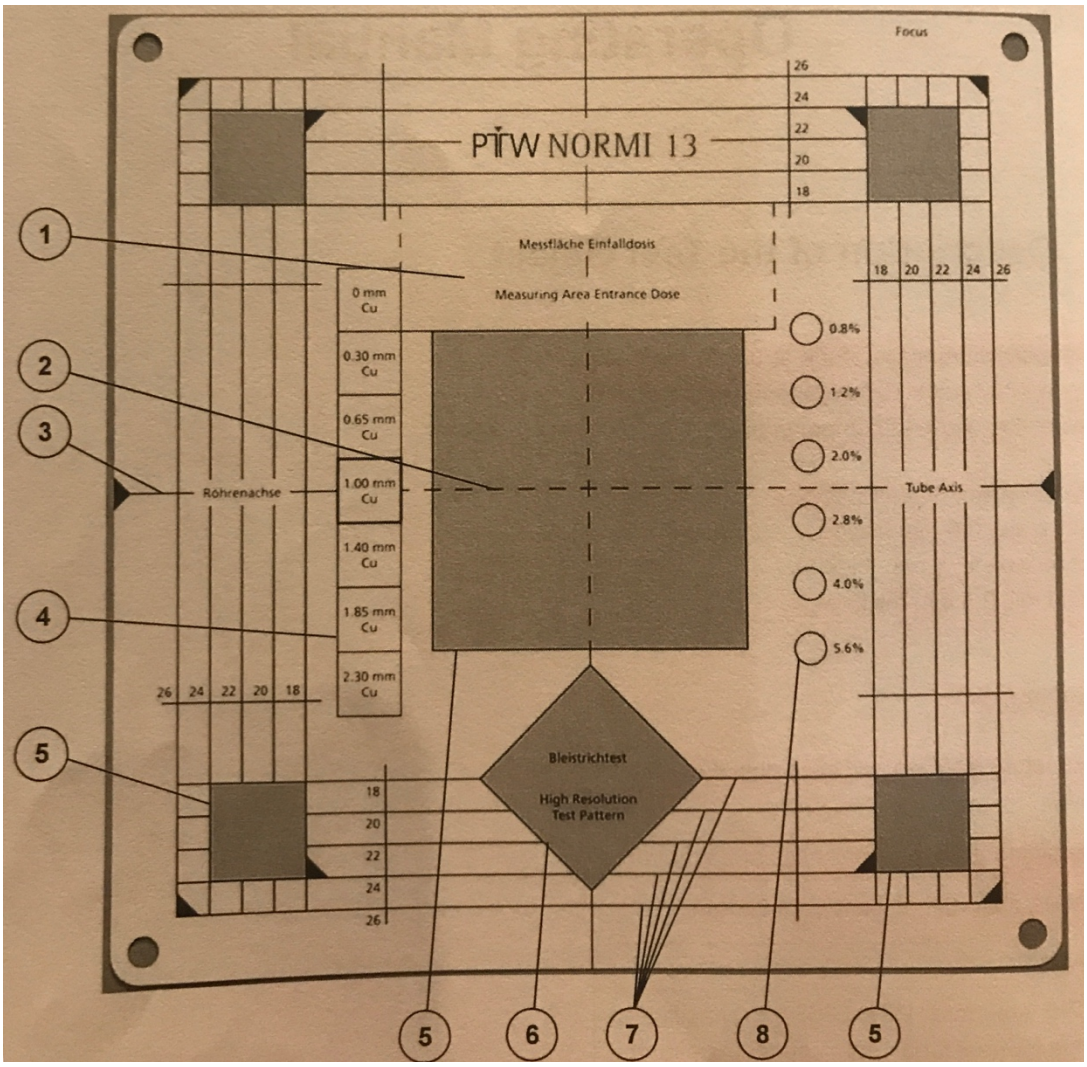

Figure 13 PTW NORMI 13 phantom suggested by Agfa manufacture to conduct exposure index, pixel vale, contrast resolution, and spatial resolution, and contrast resolution .Source (PTW-Freilburg, 2015)

1.Dose measurement area
2.Crosshairs for central alignment
3.X-ray tube axis
4.Dynamic step (contrast test)
5. Signal normalization area(uniformity test)
6. Spatial resolution test area (test pattern)
7. Radiation-absorbing line
8. Contrast resolution test (low contrast)

3.2 Methods

3.2.1 X-Ray machine calibration

In all measurements without the Normi-13 phantom, both calibration and actual tests, a filter was used. This filter consists of sandwiched Cu and Al, with thicknesses 1.5 mm and 1.75 mm respectively. Both the digital detector manufacture (Agfa) and task group 85 recommend that filters be used in order to make the x-ray beam harder. As stated above, the Normi-13 phantom contains its own filter.

For one of the tests (the Linear Response Test), calibration was required. For this, the digital detector was placed above a barrier that is made of lead. On the floor of the x-ray room at the Kettering Medical Center tape was used to mark the digital detector's place in order to avoid any changes in placement during the experiment. The collimation of the x-ray head was adjusted to fit the size of the digital detector. Then the digital detector was removed and the solid-state detector, attached to the Unfors Xi dosimeter reader, was placed at the detector location.

On the display screen of the computer attached to the x-ray unit, the machine was set on examination test mode and abdominal image. The energy of the x-ray unit was adjusted by altering the mAs for an exposure until the dose of radiation reached $\cong 10\ \mu$Gy according to the solid state detector calibration system. After the dose reached $\cong 10\ \mu$Gy the solid detector removed. Then, all the following tests were conducted with digital imaging detector.

3.2.2 Existing QA Test Routine

As stated earlier, no well-defined set of QA tests exists for DR detectors for use under various situations. At Kettering Hospital, the most comprehensive set of tests is provided by the manufacturer of the DR devices (Agfa). This set of tests is primarily meant to be used when a hospital initially receives the detector, to verify that it meets specifications before beginning to use it in clinical situations. This set of tests is fairly comprehensive and requires over 90 minutes to conduct. Thus, they are not efficient for use on a routine basis. One of the goals of this thesis was to develop a smaller, more efficient set of tests that evaluate the most likely issues that might arise with digital detectors. In order to compare the two sets of tests, in this section I will briefly describe the tests as provided in the Agfa manual (Agfa, 2015), and which ones were used, modified, or not used in the new set. The next section will describe in more detail the new set of tests that I chose and evaluated.

Table 3 lists each of the 9 tests Agfa recommends. The table also contains a column indicating whether the corresponding test is used in some fashion in the new set of proposed tests. Many of these tests use the Normi-13 phantom.

The first test is a sensitivity check to determine that the pixel value index (PVI) in the center of digital image falls within the recommended range under a standard set of conditions. The second test is a spatial resolution check. Under high contrast conditions,

the test determines the number of line pairs per millimeter (Lp/mm). The specific passing value depends on the actual device being tested

Manufacturer Test	New Routine
Sensitivity	**Not done**
Spatial Resolution	**Unchanged**
Low Contrast	**Unchanged**
Dynamic Range	**Unchanged**
Uniformity	**Modified**
True Size	**Not done**
Defect Pixel Mapping	**Not done**
Flat Field	**Not done**
Clipping Level	**Not done**

Table 3 Manufacturer Tests vs. New Routine

The third test is a low contrast test to verify that the detector can distinguish regions

which have a very small difference in intensity compared to the background intensity. The fourth test is a dynamic range test that examines PVI values for a range of material thicknesses on the phantom. A high ratio for PVI values from different regions indicates that the dynamic range is sufficient.

The fifth test is a uniformity test to verify that all regions of the detector produce similar PVI values. It measures PVI values at nine locations on the detector, in a 3x3 grid. The sixth test is a true size check that measure the dimensions of a test Cu-plate. The size as reported by the digital detector must match the predicted size of the Cu-plate after accounting for x-ray machine geometry.

The seventh test is defect pixel mapping test which exposes all the pixels to a dose, and looks for those that don't respond accurately. This test requires more time than the other tests. The eighth test is a flat field test, to assure that a uniform grey image is produced. In order to pass the test the image should appear with no white borders. Finally, a clipping level check is performed to make sure that excessively high or low doses are handled properly by the device and the software.

3.2.3 Description of Tests

3.2.3.1 Uniformity Test

The energy was set to 75 kV for stationary unit room 7 and 76 kV for all portable units. The stationary units accepts 75 kV but the portable units do not so 76kV was used instead. It is not expected that a 1 kV difference will have a large impact on the

experimental results.

For each digital imaging detector, the average pixel value and noise (SD) was recorded for each of the 5 regions of the detector as shown in Figure 14. Note that this differs from the uniformity test specified in the Agfa manual, where 9 regions were used.

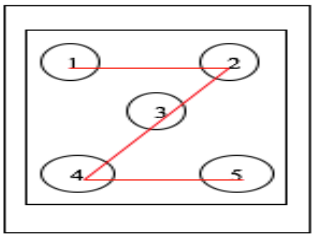

Figure 14 z pattern (uniformity test)

The uniformity of the field was determined by the following equation:

Range = Region with max avg. pixel value – Region with min avg. pixel value

$$\text{The uniformity of pixel value} = \frac{Range}{Avrage}$$

The Agfa manufacture sets the acceptance value for uniformity to be a value of 10%.

The digital imaging detector DX-D 40 was tested in combination with x-ray portable units A, B, C and fixed x-ray unit in room 7. However, digital imaging detector DR 14s was tested only with the portable A x-ray unit.

3.2.3.2 Low Contrast Test

The Normi 13 Phantom was placed above the digital imaging detector. In the low contrast test, region 8 of the Normi 13 phantom was used (Fig. 13). For this, the number of round regions that are distinguishable are counted. The manufacture indicates that to pass this test four circles should be distinguishable by visual inspection. Figure 15 shows an expanded view of the relevant region of the Normi 13 phantom, and Figure 16 presents the type of image that results.

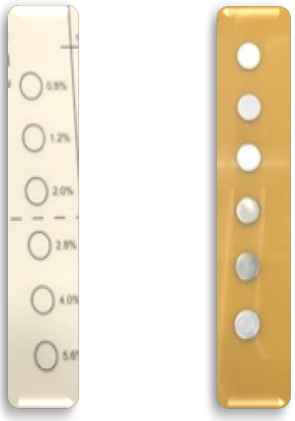

Figure 15 a part of Normi 13 phantom that has a five-objects made from aluminum each one has different thickness to test low contrast of digital imaging detector

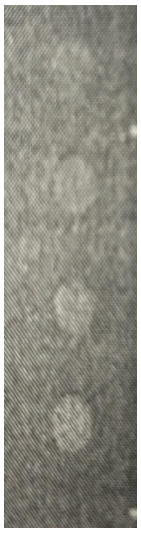

Figure 16 low contrast test four holes visible to pass source Agfa manufacture manual

3.2.3.3 Spatial Resolution Test

The Normi 13 Phantom was placed above the digital imaging DR 14s detector. In the spatial resolution test, the number of line pairs per mm, Lp/mm, was evaluated by visual inspection at 4-8x magnification. This test used region 6 of the Normi-13 phantom (Fig. 13), which contains multiple sets of x-ray opaque lines separated by varying gaps.

Acceptable values given by Agfa manual depend on the specific digital detector. However, for both of the detectors used in this thesis, the passing score is 2.5 Lp/mm or greater. An expanded view of the relevant region of the Normi-13 phantom is shown in Figure 17.

Figure 17 Test pattern that used to measure contrast (image from test object Normi 13 phantom)

3.2.3.4 Dynamic Range Test

The dynamic range test uses section 4 of the Normi-13 phantom (Fig. 13). Here the phantom contains seven squares of varying thickness of Cu, ranging from 0 mm to 2.3 mm (Figure 18). These regions are also given labels from Step 1 (no Cu) to Step 7 (max thickness Cu). The lesser thicknesses produce darker images and higher PVI values. The pixel value index (PVI) and noise (SD) was determined and recorded for each region.

In order to analyze this test, additional labels are assigned to 3 of the 7 regions. PVI 1 refers to the region with the thickest Cu (which corresponds to the lightest region on the image, which corresponds to the lowest PVI value). PVI 2 is the middle of the 7 regions, and PVI 3 is the region with no Cu. Then, the ratios PVI 3/PVI 1 and PVI 2/PVI 1 are calculated. In order to pass, the PVI 3/PVI 1 ratio must be greater than 2.0, and the PVI 2/PVI 1 ratio must be greater than 1.5.

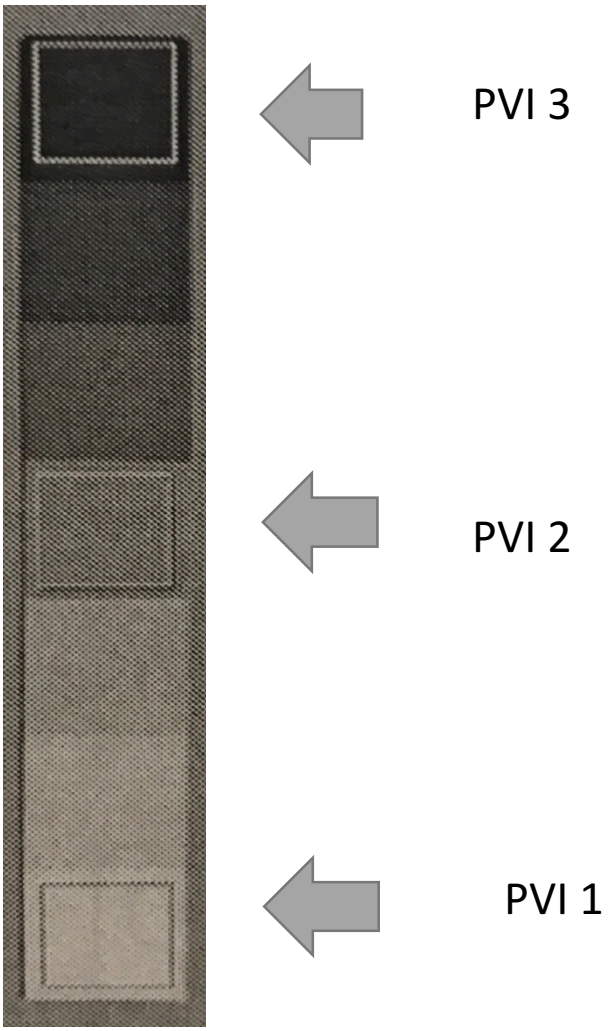

Figure 18 Pixels value for the Dynamic Range Test. Source Agfa manufacture manual

3.2.3.5 Linear Response Test

The fifth test doesn't correspond to any of the tests listed in the Afga manual. It is called a linear response test, and the goal of this test was to determine relationships between dose, in the sense of energy output from the x-ray machine, and the various readings from the digital imaging detectors. The Normi-13 phantom was not used for this test. Here, a

range of mAs values were used on the x-ray machine. First, a calibration was performed by measuring the dose in μGy using the solid state detector for a setting of 10 mAs on the x-ray machine. For each of the other mAs settings, the dose in μGy was calculated by assuming linear scaling. The response of the digital imaging detector was recorded for each mAs setting. The Exposure Index (EI) and average PVI and SD for the entire detector area were recorded. The same process was conducted for the following combinations of kV and machine: (1) 65 kV and Room 7 x-ray machine; (2) 75 kV and Room 7; and (3) 76 kV and portable A.

4. Results

4.1 Uniformity Test

Table 4 presents the average pixel value and noise of the uniformity test under for all 5 regions for all 5 detector/x-ray machine combination. Table 5 summarizes this data and presents the uniformity calculation. The most important finding is that for each detector/x-ray machine combination, the average pixel value is very consistent across all 5 regions, resulting in uniformity values under 2% in all cases. The passing score only required 10% uniformity. The noise within a region was also quite consistent under all regions and combinations.

Detector DX-D 40									**Detector DR 14s**	
Z pattern value	***Portable A***		***Portable B***		***Portable C***		***Room 7***		***Portable A***	
	Pixel value	*Noise*	*Pixel value*	*Noise*	*Pixel value*	*Noise*	*Pixel value*	*Noise*	*Pixel value*	*Noise*
1	41432	86	28215	93	34613	72	35288	71	45099	83
2	41387	100	28554	97	35085	85	35170	70	45148	87
3	41074	87	28389	93	34258	60	34797	66	45070	90
4	41527	94	28639	95	34750	80	35153	72	45080	91
5	41791	104	28550	94	34241	67	34998	71	45048	86

Table 4 Uniformity (z pattern method) test by using two digital detectors 1) DX-D 40 with x-ray units Portable A, Portable B, Portable C, and Room 7. 2) DR-14 S in x-ray unit Portable A

	Detector DX-D 40				Detector DR 14s
	Portable A	Portable B	Portable C	Room7	Portable A
Average	41432	28550	34389	35081	45189
Range	657	424	665	491	490
Uniformity	0.015	0.014	0.019	0.013	0.010

Table 5 The Average, the range and the uniformity for the uniformity test By using two detectors 1) DX-D 40 with x-ray units Portable A, Portable B,, Portable C, and Room 7. 2) DR 14s with x-ray unit Portable A

The average pixel values for each detector/x-ray machine combination tend to differ. For example, the readings from Portable A, for both detectors, tend to be higher than PVI values for the other x-ray machines. These differences are simply due to the fact that no attempt was made to standardize these readings, since the primary purpose of the test was to compare one region of the detector with another region of the detector.

4.2 Low Contrast Test

Table 6 shows the number of circles detected under various detector/x-ray machine combinations. In all cases, 4 circles were visible, which indicates a passing score.

	Detector DX-D 40				Detector DR 14s
	Portable A	***Portable B***	***Portable C***	***Room7***	***Portable A***
Low Contrast Resolution Holes visible	4	4	4	4	4

Table 6 Low Contrast Resolution Test number of Holes visible and High Contrast Resolution Ip/mm by using two digital detectors 1) DX-D 40 with x-ray units Portable A, Portable B, Portable C, and Room 7. 2) DR-14S with x-ray unit Portable A

4.3 Spatial Resolution Test

The spatial resolution test gave a value of 2.8 Lp/mm for digital imaging detector DX-D 40 with all portables units as well as for digital detector DR 14s with the portable A x-ray unit (Table 7). With the room 7 x-ray unit, the DX-D 40 detector gave a value of 3.1 Lp/mm. Base on Pixel pitch value 140 μm and 148 μm , we expect the spatial resolution to be 2.8 Lp/mm and 3.1 Lp/mm .Acceptable Values are 2.5 Lp/mm or greater for both detectors, so these are passing values.

	Detector DX-D 40				**Detector DR 14s**
	Portable A	Portable B	Portable C	Room7	Portable A
Lp/mm	2.8	2.8	2.8	3.1	2.8

Table 7 Contrast Resolution Lp/mm by using two digital detectors 1) DX-D 40 with x-ray units Portable A, Portable B, Portable C, and Room 7. 2) DR-14S with x-ray unit Portable A

4.4 Dynamic Range Test

Table 8 displays the PVI values and SD from the dynamic range test for steps 1-7. All detector/x-ray machine combinations show the expected decrease in PVI values as step number increases, corresponding to increasing Cu thickness. Similar to the results from the uniformity test, different detector/x-ray machine combinations produced different average PVI values. Also note that the noise increases as the step number moves to lighter (less exposed) values. Remember that this is the noise compared to a standardized value

for the signal, and so it could be thought of as a noise-to-signal ratio.

Step	Detector DX-D 40								Detector DR 14s	
	Portable A		***Portable B***		***Portable C***		***Room 7***		***Portable A***	
	Pixel Value	*Noise*	*Pixel Value*	*Noise*	*Pixel Value*	*Noise*	*Pixel Value*	*Noise*	*Pixel Value*	*Noise*
1	60778	41	47937	53	52002	0	52383	31	62184	21
2	52499	96	39571	98	45560	87	45189	75	55018	56
3	46081	103	33084	107	39218	91	39277	72	46152	62
4	40875	119	27328	122	34054	103	34445	87	44299	81
5	35826	168	22770	158	29031	147	29610	124	39449	112
6	31166	213	18099	257	24436	212	25019	135	34770	141
7	27890	484	14981	564	21155	398	21514	256	31321	373

Table 8 The Dynamic Range Test from black to white by using two digital detectors 1) DX-R 40 with x-ray units Portable A, Portable B, Portable C, and Room 7. 2) DR-14S with x-ray unit Portable A

In portable C, a surprising result from the noise data is a noise value of zero in the first black step. Since each of these readings occur over many pixels, it is unlikely that every pixel in the square for step 1 would have the exact same PVI value. Thus this is probably either a user error or a software error.

The ratios of PVI values for steps 1, 4, and 7 are presented in Table 9. Passing values were obtained all combinations except: (1) PVI 3/PVI 1 ratio for detector DR 14s with portable A; and (2) PVI 2/PVI 1 ratio for both detectors with Portable A. However, these non-passing ratios were within 10% of acceptable ratios, and so the failure isn't considered serious.

PVI Range	Detector DX-D 40				Detector DR 14s
	Portable A	Portable B	Portable C	Room7	Portable A
PVI 3/PVI1	2.179	3.199	2.458	2.520	1.985
PVI2/PVI1	1.465	1.824	1.609	1.601	1.414

Table 9 pixel value index from The Dynamic Range Test from black to white by using two digital detectors 1) DX-D 40 with x-ray units Portable A, Portable B, Portable C, and Room 7. 2) DR-14S with x-ray unit Portable A

4.5 Linear Response Test

4.5.1 65 kV, Room 7

Table 10 shows the results of the linear response test for digital imaging detector DR 14s with a 65 kV x-ray beam over 2-50 mAs. As expected, exposure index and pixel value index (PVI) increase as mAs increases. Recall that exposure is proportional to mAs. However, noise dropped from 199 to 40. The most interesting finding is that while noise decreases as mAs increases, the relative improvement becomes less and less, indicating that one achieves diminishing returns as one continues to increase mAs.

Figure 19 shows a graph of Exposure Index vs dose. Exposure index rose linearly. The AAPM guideline of having an R^2 for this plot over 0.999 was passed. Figure 20 shows a graph of pixel value index vs dose, but plotted on a logarithmic scale. This shows a linear relationship when plotted this way. The proportionality of PVI with log dose was not known before this data was assembled and plotted. Remember that PVI is a proprietary

calculation by the detector manufacturer. Figure 21 plots the noise vs dose. Here one can see the leveling off of noise values as dose increases.

Detector DR 14s				
Room 7				
Tube current (mAs)	**Dose (µGy)**	**EI**	**PVI**	**Noise**
2	2.49	85	22212	199
3.2	3.98	147	27045	149
6.3	7.84	307	33296	108
10	12.45	491	37422	84
12.5	15.57	616	39397	74
20	24.91	1001	43547	58
32	39.87	1619	47665	49
50	62.29	2538	51552	40

Table 10 Evaluation of The DR 14s digital detector at 65kV.

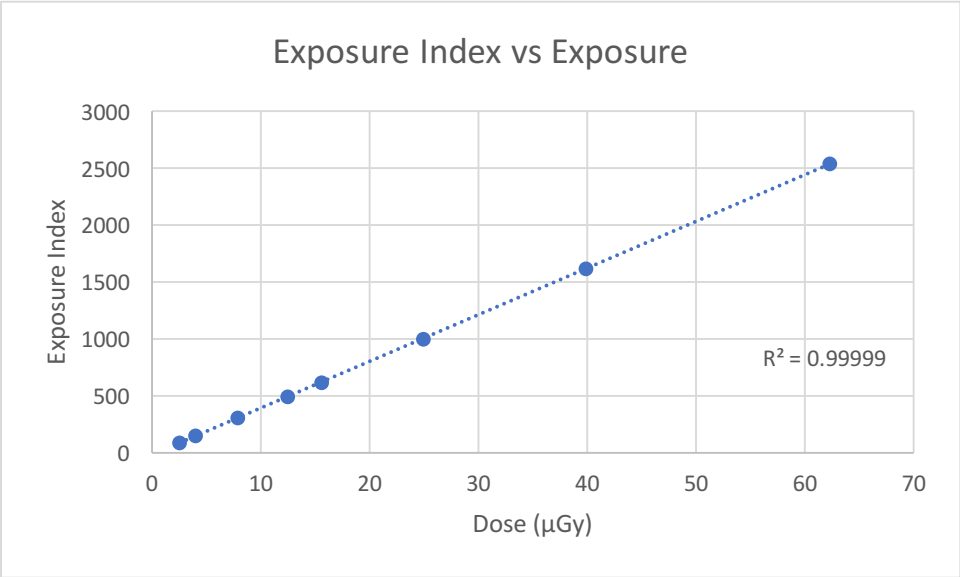

Figure 19. The exposure index for DR 14s digital detector at 65kV, Room 7

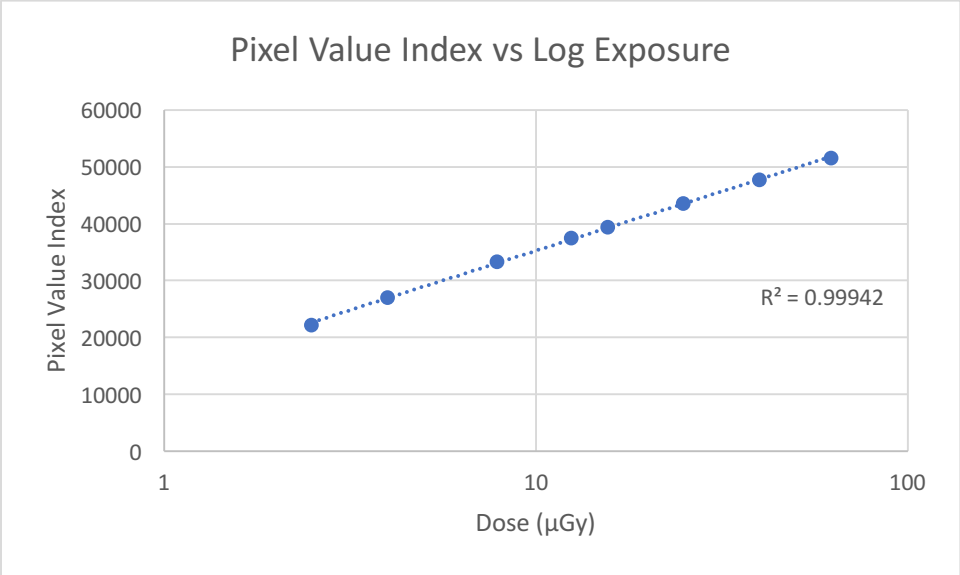

Figure 20. The pixel value index for DR 14s digital detector at 65kV, Room 7

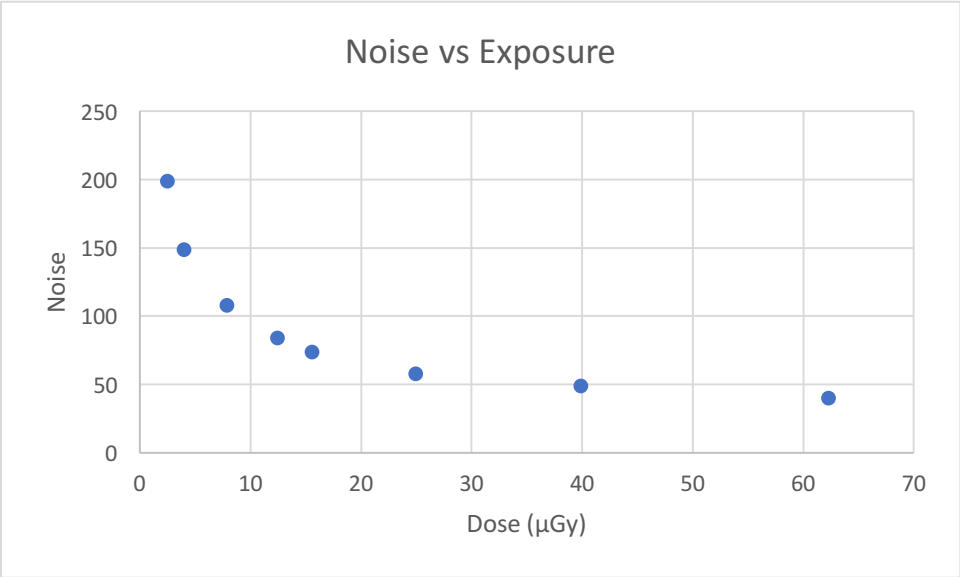

Figure 21. The noise for DR 14s digital detector at 65kV, Room 7

4.5.2 75 kV, Room 7

Plots and results for a voltage setting of 75 kV on the room 7 x-ray machine are shown in Table 11 and Figures 22, 23, and 24. The results and main points are very similar to those in section 4.5.1.

Detector DR 14s				
Room 7				
mAs	**µGy**	**EI**	**PVI**	**Noise**
0.5	0.62297129	30	13304	366
1	1.24594257	84	22020	209
2	2.49188514	197	29451	134
4	4.98377029	427	36137	59
8	9.967	892	42468	78
10	12.45942572	1119	44401	58
12.5	15.5742821	1409	46456	58
20	24.918	2266	50556	42
25	31.14856429	2841	52523	39

Table 11 Evaluation of DR 14s digital detector at 75kV, Room 7

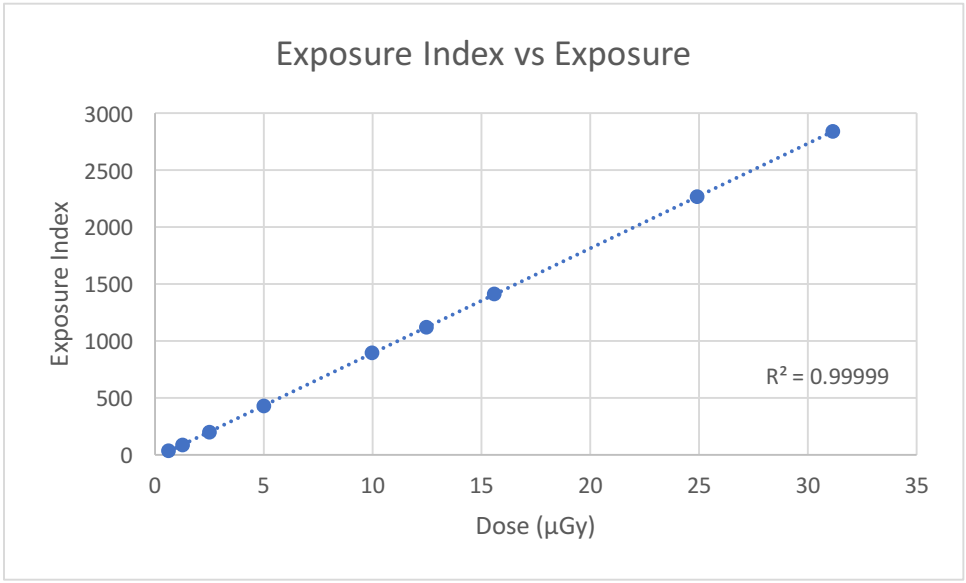

Figure 22. The exposure index for DR 14s digital detector at 75kV, Room 7

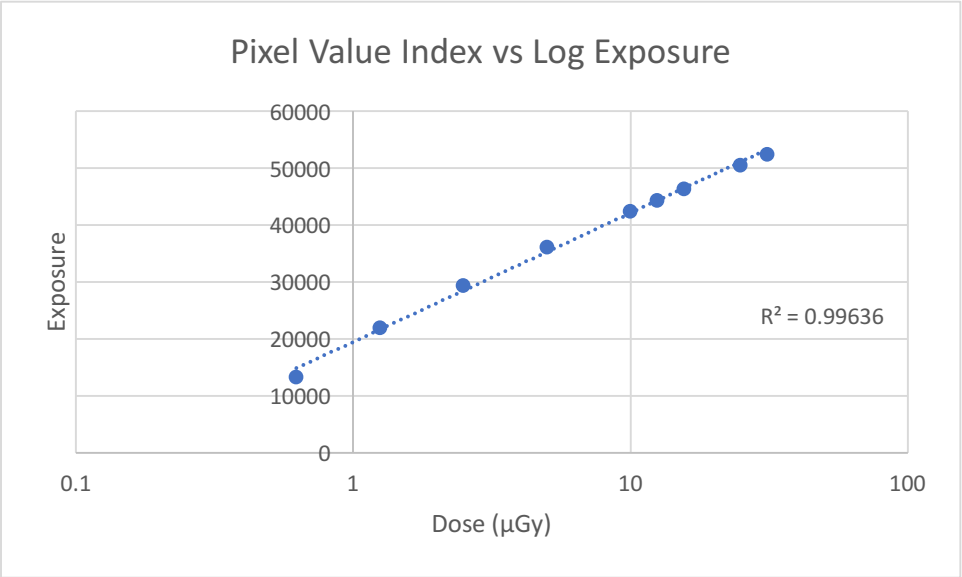

Figure 23. The pixel value index for DR 14s digital detector at 75kV, Room 7

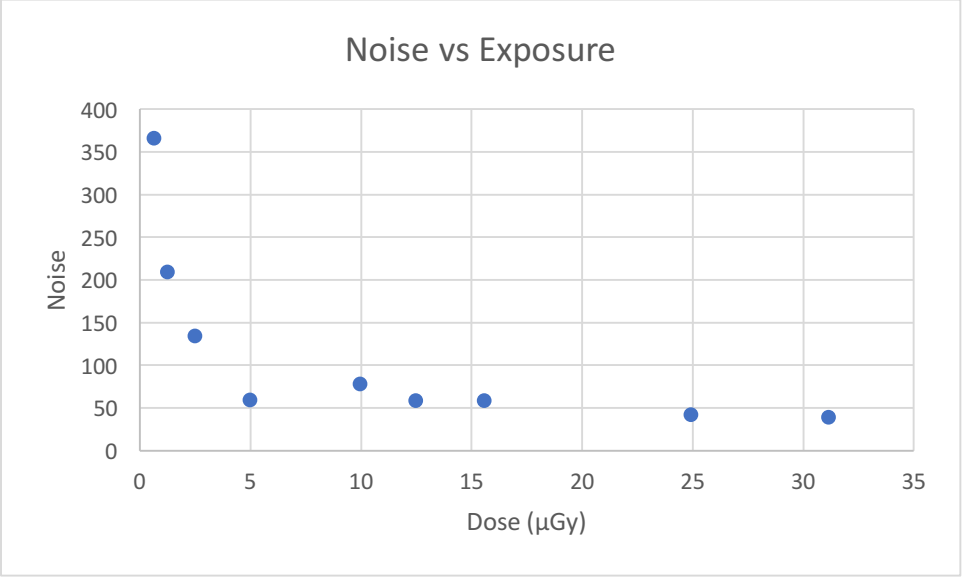

Figure 24. The noise for DR 14s digital detector in 75kV

4.5.3 76 kV, Portable A

Plots and results for a voltage setting of 76 kV on the portable A x-ray machine are shown in Table 12 and Figures 25, 26, and 27. The results and main points are very similar to those in sections 4.5.1 and 4.5.2.

Detector DR 14s				
Portable A				
Tube current (mAs)	**Dose (µGy)**	**EI**	**PVI**	**Noise**
0.5	0.622	35	14607	336
0.63	0.784	49	17468	280
1	1.245	93	22989	196
2	2.491	223	38693	126
4	4.983	483	37122	86
8	9.967	1001	43447	61
10	12.459	1261	45441	55
20	24.918	2561	51588	39

Table 12. Evaluation of DR 14s digital detector at 76kV, Portable A

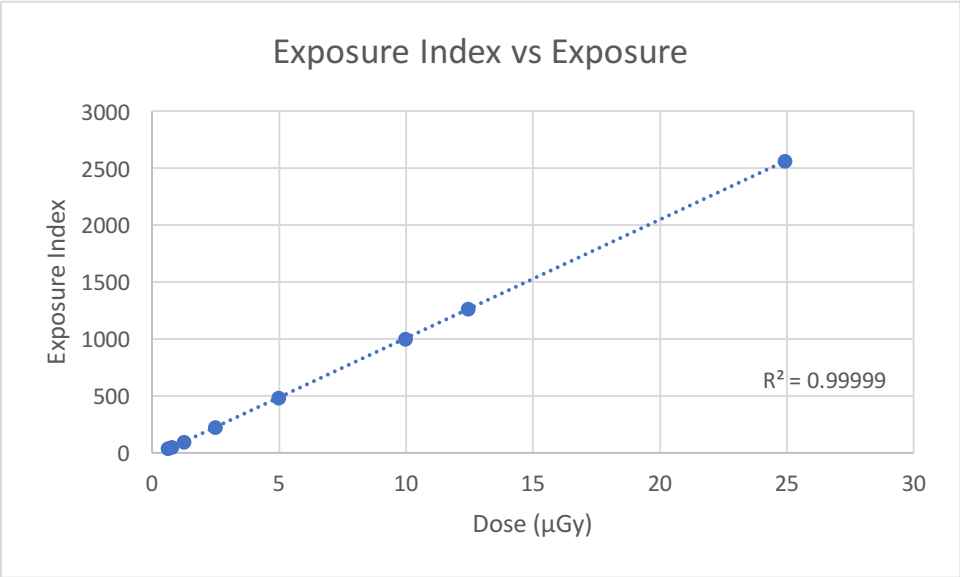

Figure 25. The exposure index for DR 14s digital detector at 76kV, Portable A

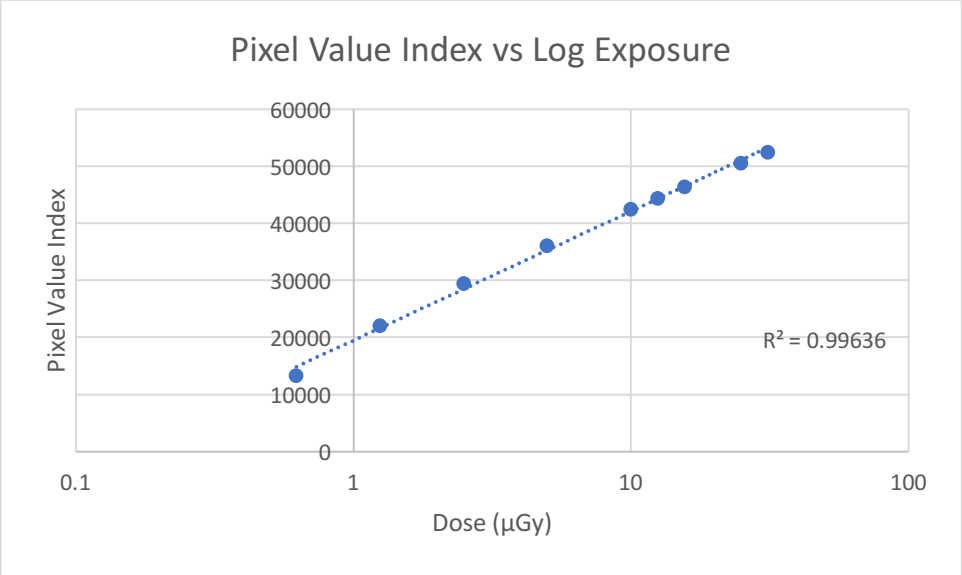

Figure 26. The pixel value index for DR 14s digital detector at 76kV, Portable A

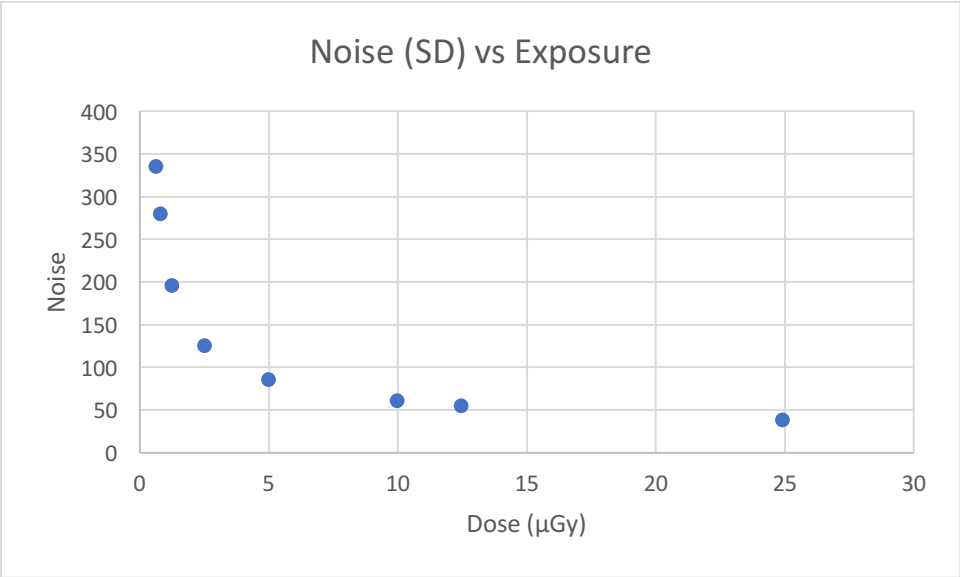

Figure 27. The noise for DR 14s digital detector at 76k, Portable A

5. Discussion and Conclusions

In quality assurance testing, the most important goal is to verify that the equipment is operating in a manner that minimizes potential harm to the patient while maximizing the medical information obtained. A secondary goal is that the quality assurance routines should be efficient because in the real world clinical setting, an overly long or laborious sequence of tests has the potential to be performed badly or less often than necessary. Thus the goal of this work was to identify a set of tests, mostly drawn from a complete set of tests suggested by the digital imaging detector device manual for initial device validation, which reveal maximum information for minimum effort when used with multiple machines and detectors. The results from this study have shown that 5 separate tests all performed well for up to 2 different detectors and 4 different x-ray machines. The uniformity test, the low contrast test, the spatial resolution test, the dynamic range test, and the linearity test combine to give a fast and convenient routine to evaluate the digital imaging detector quality and reveal potential problems.

A particularly useful finding from this work is the behavior of the noise levels as the exposure increased (Figures 21, 24, and 27). Since these should be interpreted as a noise-to-signal ratio, one can see that there is diminishing returns as one increases exposure. Choosing an exposure of say 7 or 10 μGy (for 75 or 76 kV), or 25 μGy (for 65kV) seems to provide almost all the benefit of improved signal-to-noise that one can obtain by increasing exposure. As one goes below 10 μGy the noise decreases as $\sqrt{x}$

(where x is the exposure) but the signal decreases linearly with x, and thus signal-to-noise is low at lower exposures. Choosing the optimum exposure using this data will lead to less patient exposure to radiation.

The number of lines per mm from the room 7 x-ray unit was higher than for the other x-ray units (Table 7). The digital detector DX-D 40 was expected to give the same value for all x-ray units. The reason for this is probably that using stationary x-ray unit provides some reduced machine movement.

Future work in this area should evaluate time required for this set vs complete set. The primary time savings was obtained by not performing the defective pixel mapping test. However, this also means that some detector problems might be missed, so an additional evaluation that should be done in the future is to compare detectors that function optimally vs detectors that have problems, so that one can get a better understanding of the false positive rate for this set of tests.

References

1. Al Mahbub, A., & Haque, A. (2016). X-ray Computed Tomography Imaging of the Microstructure of Sand Particles Subjected to High Pressure One-Dimensional Compression. *Materials (1996-1944)*, *9*(11), 1-17. doi:10.3390/ma9110890
2. Allisy-Roberts, P., Williams, J. R., & Farr, R. F. (2008). *Farr's physics for medical imaging*. Edinburgh: Saunders
3. Attix, F. H. (1986). *Introduction to radiological physics and radiation dosimetry*. New York: Wiley.
4. Ball, J., Moore, A. D., Turner, S., & Ball, J. (2008). *Ball and Moore's essential physics for radiographers*. Chichester, UK: Blackwell Science.
5. Bourne, R. (2010). *Fundamentals of digital imaging in medicine*. London : Springer, c2010.
6. Bushong, S. C. (2013). *Radiologic science for technologists: Physics, biology, and protection*.
7. Carter, C. E., & Vealé, B. L. (2008). *Digital radiography and PACS*. St. Louis, Mo: Mosby Elsevier.
8. Choi, J., Kim, K., & Kim, G. (2016). Image Selection Algorithm Proposal for Digital Radiography Training Simulator. *Wireless Personal Communications*, *89*(3), 833-845. doi:10.1007/s11277-016-3247-3
9. Delis, H., Christaki, K., Healy, B., Loreti, G., Poli, G., Toroi, P., & Meghzifene, A. (2017). Moving beyond quality control in diagnostic radiology and the role of the clinically qualified medical physicist. *Physica Medica*, *41*104. doi:10.1016/j.ejmp.2017.04.007
10. digital Imaging Plate (DIP) Camera for Very High Spatial Resolution, Soft X-Ray Imaging. (2007). *2007 IEEE 34th International Conference on Plasma Science (ICOPS), Plasma Science, 2007. ICOPS 2007. IEEE 34th International Conference on*, 239. doi:10.1109/PPPS.2007.4345545
11. Domadia, N., Bheda, H., Modiya, S., & Raychaudhari, C. (2017). Role of CT scan in diagnosis of HELLP syndrome: Radiologist's perspective. *International Archives Of Integrated Medicine*, *4*(2), 60-63.
12. Fauber, T. L. (2013). *Radiographic imaging & exposure*. St. Louis, Mo. : Elsevier Mosby, c2013.
13. Hall, E. J. (2000). *Radiobiology for the radiologist*. Philadelphia: Lippincott Williams & Wilkins.
14. Haus, A. G., & Jaskulski, S. M. (1997). *The basics of film processing in medical imaging*. Madison, Wis. : Medical Physics Pub., c1997.
15. Hendee, W. R., & Ritenour, E. R. (2002). *Medical imaging physics*. New York.

16. Kawashima H, Ichikawa K, Nagasou D, Hattori M. X-ray dose reduction using additional copper filtration for abdominal digital radiography: Evaluation using signal difference-to-noise ratio. *Physica Medica: PM: An International Journal Devoted To The Applications Of Physics To Medicine And Biology: Official Journal Of The Italian Association Of Biomedical Physics (AIFB)*[serial online]. February 2017;34:65-71. Available from: MEDLINE with Full Text, Ipswich, MA. Accessed October 9, 2017.
17. Liu, S., Sima, W., Yuan, T., Luo, D., Bai, Y., & Yang, M. (2017). Study on X-Ray Imaging of Soil Discharge and Calculation Method of the Ionization Parameters. *IEEE Transactions On Power Delivery*, *32*(4), 2013-2021. doi:10.1109/TPWRD.2016.2597238
18. Mettler, F. A. (2014). *Essentials of radiology*.
19. Mikla, V. I., & Mikla, V. V. (2014). *Medical imaging technology*. Amsterdam ; Boston : Elsevier, [2014].
20. Perks, T. D., Dendere, R., Irving, B., Hartley, T., Scholtz, P., Lawson, A., & ... Douglas, T. S. (2015). FILTRATION TO REDUCE PAEDIATRIC DOSE FOR A LINEAR SLOT-SCANNING DIGITAL X-RAY MACHINE. *Radiation Protection Dosimetry*, *167*(4), 552-561. doi:10.1093/rpd/ncu339
21. Perks, T. D., Dendere, R., Irving, B., Hartley, T., Scholtz, P., Lawson, A., & ... Douglas, T. S. (2015). FILTRATION TO REDUCE PAEDIATRIC DOSE FOR A LINEAR SLOT-SCANNING DIGITAL X-RAY MACHINE. Radiation Protection Dosimetry, 167(4), 552-561. doi:10.1093/rpd/ncu339
22. Reiner, Bruce I., MD. "Automating Quality Assurance for Digital Radiography." *Journal of the American College of Radiology*, vol. 6, no. 7, 2009, pp. 486-490. *OhioLINK Electronic Journal Center*, doi:10.1016/J.JACR.2008.12.008.
23. Ricketts, J. (2016). Film-Screen Radiography in Bachelor's Degree Program Curriculum. *Radiologic Technology*, *88*(2), 234-236.
24. Tian X, Yin Z, Man B, Samei E. Estimation of Radiation Dose in CT Based on Projection Data. *Journal Of Digital Imaging*[serial online]. October 2016;29(5):615. Available from: Complementary Index, Ipswich, MA. Accessed October 9, 2017.